ACS POLYMERS Au
AN OPEN ACCESS JOURNAL OF THE AMERICAN CHEMICAL SOCIETY

pubs.acs.org/polymerau

Article

Quantifying Properties of Polysaccharide Solutions

Ryan Sayko, Michael Jacobs, and Andrey V. Dobrynin*

Cite This: *ACS Polym. Au* 2021, 1, 196–205

Read Online

ACCESS | Metrics & More | Article Recommendations | Supporting Information

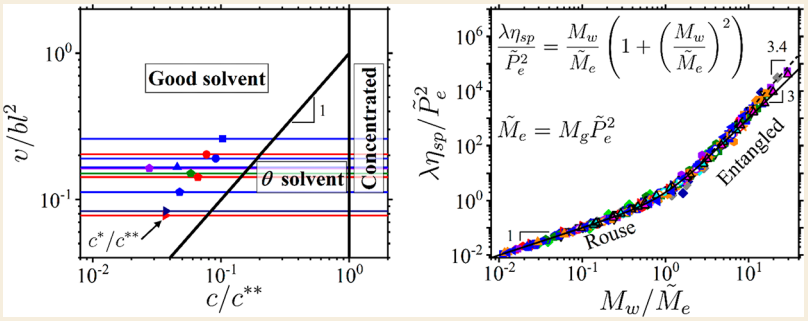

ABSTRACT: We apply a scaling theory of semidilute polymer solutions to quantify solution properties of polysaccharides such as galactomannan, chitosan, sodium carboxymethyl cellulose, hydroxypropyl methyl cellulose, methyl cellulose, xanthan, apple pectin, cellulose tris(phenyl carbamate), hydroxyethyl cellulose, hydroxypropyl cellulose, sodium hyaluronate, sodium alginate, and sodium κ-carrageenan. In particular, we obtain the molar mass of the chain segment inside a correlation blob $M_g = \hat{B}^{3/(3\nu-1)} c^{1/(1-3\nu)}$ as a function of concentration c, interaction parameter $\hat{B}$, and exponent ν. Parameter $\hat{B}$ assumes values $\hat{B}_g$, $\hat{B}_{th}$ and $M_0/N_A{}^{1/3}\, l$ for exponents ν = 0.588, 0.5 and 1, respectively, where M_0 is the molar mass of a repeat unit, l is the projection length of a repeat unit, and N_A is the Avogadro number. In the different solution regimes, the values of the $\hat{B}$-parameters are extracted from the plateaus of the normalized specific viscosity $\eta_{sp}\,(c)/M_w\, c^{1/(3\nu-1)}$, where M_w is the weight-average molecular weight of the polymer chain. The values of the $\hat{B}$-parameters are used in calculations of the excluded volume v, Kuhn length b, and crossover concentrations c^*, c_{th}, and c^{**} into a semidilute polymer solution, a solution of overlapping thermal blobs and a concentrated polymer solution, respectively. This information is summarized as a diagram of states of different polysaccharide solution regimes by implementing a v/bl^2 and c/c^{**} representation. The scaling approach is extended to the entangled solution regime, allowing us to obtain the chain packing number, $\tilde{P}_e$. This completes the set of parameters $\{\hat{B}_g, \hat{B}_{th}, \tilde{P}_e\}$ which uniquely describes the static and dynamic properties of a polysaccharide solution.

KEYWORDS: *scaling, polysaccharides, polymer solutions, solution viscosity*

INTRODUCTION

Among the diverse family of biomacromolecules, polysaccharides, consisting of sugar repeat units linked by glycosidic bonds, are the most prolific and versatile biopolymers.[1,2] The solution properties of such biopolymers are determined by the type of functional groups (e.g., hydroxyl, amino, and carboxyl groups), solution pH, and polymer and salt concentrations.[3−10] The abundance of polysaccharides in nature and the ability to control their solution properties[11,12] fostered their use in food packaging,[13−15] cosmetics,[16,17] and paper production.[18,19]

The importance of polysaccharides in industrial applications[20−22] combined with the quest to understand the fundamental properties of biopolymer solutions has fueled extensive studies of this class of biomacromolecule during the past 40 years.[16,23−32] In particular, taking a page from studies of solutions of synthetic polymers, the dependence of viscosity on the concentration and molecular weight of polysaccharide solutions was rationalized by adopting the c/c^* representation, quantifying the proximity of the solution concentration c to the polymer overlap concentration, c^*.[24,26,33−48] While this approach works well close to the overlap concentration, it fails at high polymer concentrations when the scaling relationship between the solution correlation length ξ and the number of polymer repeat units inside it changes from that at the overlap concentration. For example, in solutions of neutral polymers in a good solvent, this happens when the thermal blobs begin to overlap at a concentration $c \approx c_{th}$. At higher polymer concentrations, $c > c_{th}$, the solution properties are similar to those in a θ solvent for the polymer backbone, and the statistics of a chain is qualitatively different from that

Received: September 1, 2021
Revised: October 8, 2021
Accepted: October 11, 2021
Published: October 29, 2021

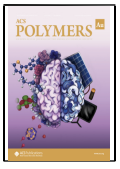

near $c \approx c^*$.[49] To address this issue, we have recently developed a generalized scaling approach[50−52] which provides a means to obtain crossover concentrations into different solution regimes and system parameters describing chain statistics at different length scales by using the concentration dependence of the solution viscosity. Here, we adapt this approach to describe solution properties of chitosan,[36] sodium hyaluronate,[37,46,53] sodium alginate,[47] sodium κ-carrageenan,[47,54] xanthan,[44,55] galactomannan,[38,42,48] and various cellulose derivatives.[34,47,56,57] Specifically, for these solutions of polysaccharides, we calculate the interaction parameters, crossover concentrations, and chain packing parameter describing chain entanglements in solutions of overlapping chains. To illustrate the universality of the developed approach, the viscosity data for all systems are represented as a universal function of the ratio M_w/M_e of the weight-average molecular weight, M_w, and the molecular weight between entanglements, M_e, the explicit concentration dependence of which is obtained for each solution regime.

The rest of the paper is organized as follows. First, we overview the scaling model of polymer solutions and illustrate how to quantify scaling relations and to find numerical coefficients connecting the solution correlation length with the number of repeat units in it. Next, we detail our approach by applying it to systems of sodium carboxymethyl cellulose and apple pectin. Finally, we analyze the relationships between the studied polymer/solvent pairs and the obtained system parameters.

OVERVIEW OF THE SCALING MODEL

The scaling model relies on the existence of a single characteristic length scale: the solution correlation length, ξ. All interactions are assumed to be screened beyond this length scale such that a polymer chain with degree of polymerization N behaves as an ideal chain of correlation blobs, each consisting of g repeat units, and has size

$$R = \xi(N/g)^{0.5} \tag{1}$$

Within the correlation blob, the polymer statistics is governed by polymer−polymer and polymer−solvent interactions determining the relationship between the solution correlation length and the number of repeat units g with projection length l in a correlation blob

$$\xi = lg^{\nu}/B \tag{2}$$

The numerical coefficient B and exponent ν are determined by the solvent quality for the polymer backbone, chain Kuhn length b, and strength of interactions at different length scales starting from the solution correlation length down to length scales smaller than the thermal blob size, D_{th}.

In semidilute polymer solutions in good solvents, the exponent ν is equal to 0.588, 0.5, and 1, and the B-parameter assumes values B_g, B_{th} and 1 in the different solution regimes. In particular, the parameter B_g characterizes the chain properties on length scales larger than the thermal blob size, D_{th} (see Figure 1), and is expressed in terms of the ratio of the repeat unit projection length l, Kuhn length b, and excluded volume v as

$$B_g = l(lb)^{3\nu-2}v^{1-2\nu} \tag{3}$$

which follows directly from the Flory expression for chain size in a good solvent[49] when rewritten for the exact exponent of a self-avoiding walk $\nu = 0.588$. Thus, the B_g parameter decreases with increasing value of the excluded volume v and smaller values of this parameter correspond to a better solvent for the polymer backbone. On the length scales smaller than the thermal blob size, the sections of a chain are ideal corresponding to exponent $\nu = 0.5$, and the parameter B_{th} is defined as

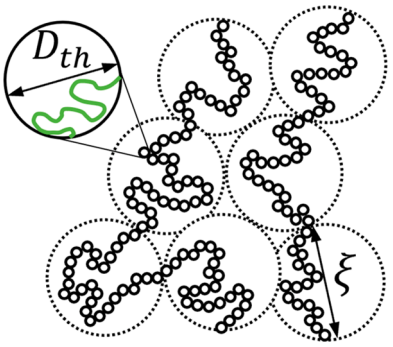

Figure 1. Schematic representation of the different length scales of semidilute polymer solutions in a good solvent. ξ is solution correlation length, and D_{th} is the thermal blob size.

$$B_{th} = (l/b)^{0.5} \tag{4}$$

Finally, on length scales smaller than the Kuhn length, b, chain segments are rod-like, resulting in $B = 1$ and exponent $\nu = 1$.

Note that, in a θ solvent for the polymer backbone, the parameter B assumes values B_{th} and 1, while the exponent ν = 0.5 and 1.

Taking into account the space-filling condition of the correlation blobs such that the repeat unit concentration inside the blobs is equal to the solution concentration

$$c = g/\xi^3 \tag{5}$$

and using eq 2, we obtain the following expressions for the correlation length

$$\xi = lB^{1/(3\nu-1)}(cl^3)^{\nu/(1-3\nu)} \tag{6}$$

and the number of repeat units per correlation blob

$$g = B^{3/(3\nu-1)}(cl^3)^{1/(1-3\nu)} \tag{7}$$

as functions of the concentration of repeat units.

The expression for solution viscosity in the framework of the scaling approach is derived by assuming that the screening of hydrodynamic interactions between chains occurs at the length scales on the order of solution correlation length ξ.[49,58,59] This assumption results in the solution specific viscosity η_{sp} to have the following crossover expression between the Rouse and entangled regimes[50]

$$\eta_{sp} = N_w\left(1 + \left(\frac{N_w}{\tilde{N}_e}\right)^2\right)\begin{cases} g^{-1}, & \text{for } c \le c^{**} \\ cbl^2, & \text{for } c^{**} < c \end{cases} \tag{8}$$

where $c^{**} = 1/lb^2$ is the concentration at which the correlation length is equal to the Kuhn length, $\xi(c^{**}) = b$, N_w is the weight-average degree of polymerization, and $\tilde{N}_e$ is the number of the repeat units per entanglement strand which, for the Kavassalis−Noolandi conjecture[60−62] for chain entanglements (see Supporting Information), is equal to

https://doi.org/10.1021/acspolymersau.1c00028
ACS Polym. Au 2021, 1, 196−205

$$\tilde{N}_e = \tilde{P}_e^2 \begin{cases} g, & \text{for } c \le c^{**} \\ c^{-2}(lb)^{-3}, & \text{for } c^{**} < c \end{cases} \quad (9)$$

The accent character "$\tilde{...}$" is used to indicate that the system polydispersity is included in the definition of the number of repeat units per entanglement strand N_e and packing number P_e (the number of entangled strands required for a section of a chain with N_e repeat units to entangle). Using eq 9, eq 8 can be rewritten in terms of the number of repeat units per correlation blob g and weight-average degree of polymerization N_w as[50]

$$\lambda\eta_{sp} = \frac{N_w}{g}\left(1 + \left(\frac{N_w}{\tilde{P}_e^2 g}\right)^2\right) \quad (10)$$

where the rescaling factor $\lambda = 1$ for $c \le c^{**}$ and $\lambda = clb^2 = c/c^{**}$ for $c > c^{**}$. This rescaling is required due to the different concentration dependence of the number of repeat units per correlation blob g and strand degree of polymerization $\tilde{N}_e$ in the concentrated solution regime $c > c^{**}$. The number of repeat units per correlation blob is calculated by using eq 7 for $c \le c^{**}$ and $g = B_{th}^{-2}(c^{**}/c)^2$ for concentration range $c > c^{**}$.

The Kavassalis−Noolandi expression (eq 9) for degree of polymerization of the entangled polymer strands breaks down in a marginally good or θ solvent for the polymer backbone for which $B_g > B_{th}^{4-6\nu}$, where $\nu = 0.588$. In this case, one must use the Rubinstein−Colby expression for the concentration dependence of N_e[63−65] and the generalized expression for solution specific viscosity[50] (see Supporting Information).

ANALYSIS OF EXPERIMENTAL DATA

The scaling approach developed above is easy to apply to solutions of synthetic polymers for which polymer composition and chemical structure are simple enough. However, in the case of biopolymers, due to the uncertainty of the degree of substitution of the functional groups and the complexity of the repeat units, it is more convenient to use molecular weight M_g (g/mol) of a strand inside a correlation blob instead of the number of repeat units g and substitute dimensionless concentration cl^3 by solution concentration c in terms of the mass per liter of solution (g/L). Maintaining the same units on both sides of eq 7, it can be rewritten as follows

$$M_g = \hat{B}^{3/(3\nu-1)} c^{1/(1-3\nu)} \quad (11)$$

where the $\hat{B}$-parameters have dimensions of $[(g/L)^{1/3}\ (g/mol)^{\nu-1/3}]$ or $[(g/mol)^{\nu}\ (mol/L)^{1/3}]$. In writing eq 11, we use the accent character "$\hat{...}$" to indicate that the $\hat{B}$-parameters presented here are different from the ones introduced in the previous section. Note that this modification does not change the form of eq 10 because the ratio $N_w/g = M_w/M_g$ is dimensionless. As before, we can use the space-filling condition of the correlation blobs,

$$c = M_g/\xi^3 N_A \quad (12)$$

to calculate the correlation length

$$\xi = \hat{B}^{1/(3\nu-1)} c^{\nu/(1-3\nu)} N_A^{-1/3} = M_g^{\nu}/\hat{B}N_A^{1/3} \quad (13)$$

where N_A is the Avogadro number. Comparing eqs 2 and 13, we can write down a general relationship between the B- and $\hat{B}$-parameters

$$B = l\hat{B}N_A^{1/3}/M_0^{\nu} \quad (14)$$

where M_0 is the molar mass of the repeat unit.

Figure 2 shows the concentration dependence of the molar mass M_g of a chain segment inside a correlation blob in the different solution regimes bounded by the chain overlap concentration c^*, thermal blob overlap concentration c_{th}, and the crossover concentration to the concentrated solution regime c^{**}. The polymer overlap concentration c^* is determined by taking eq 11 in the limit of $M_g = M_w$,

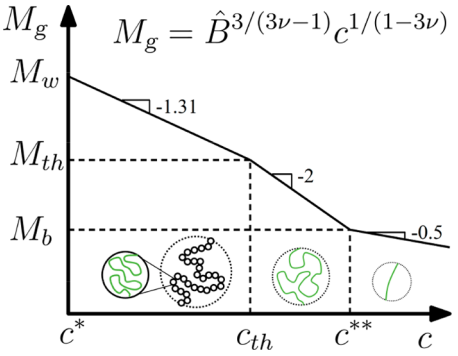

Figure 2. Concentration dependence of the molecular weight of a chain segment in a correlation blob, M_g, in semidilute polymer solutions $c > c^*$ with crossover concentrations c_{th} − thermal blob overlap concentration, and c^{**} − crossover concentration to concentrated solution regime. M_{th} is the molar mass of the segment of a chain within a thermal blob. M_b is the molar mass of the Kuhn segment. Insets show chain conformations at the correlation length scale in different concentration regimes. Logarithmic scales.

$$c^* = \hat{B}^3 M_w^{1-3\nu} \quad (15)$$

where $\nu = 0.588$ and $\hat{B} = \hat{B}_g$ for a good solvent and $\nu = 0.5$ and $\hat{B} = \hat{B}_{th}$ in the case of a θ solvent. By equating eq 11 in the regimes corresponding to the parameters $\hat{B}_g$ and $\hat{B}_{th}$ at the thermal blob overlap concentration c_{th}, one obtains

$$c_{th} = \hat{B}_{th}^3 (\hat{B}_{th}/\hat{B}_g)^{1/(2\nu-1)} \quad (16)$$

with exponent $\nu = 0.588$.

However, to obtain polymer Kuhn length, b, the excluded volume, ν, and the crossover concentration to the concentrated solution regime, c^{**}, it is necessary to calculate the average molecular weight M_0 and projection length l of a repeat unit, taking into account the degree of substitution of functional groups. If the structure of the biopolymer backbone and the degree of substitution of substituents is well-defined and characterized, then one can use these parameters to estimate M_0 and l as explained in Section S3 of the Supporting Information.

In particular, for any biopolymer that has a repeat unit that consists of single $\beta(1 \to 4)$ linked D-glucose units, then we use repeat unit projection length $l = 0.54$ nm.[66] For biopolymers with repeat units of one $\beta(1 \to 4)$ linked unit and one $\beta(1 \to 3)$ linked unit, we use $l = 0.99$ nm (estimated from ChemDraw). The values of M_0 and l used for each data set can be found in Table 1. Then, using eqs 14 and 16 and the definitions of the dimensionless B-parameters, the Kuhn length b, excluded volume ν, and concentration c^{**} can be calculated as follows

$$b = l/B_{th}^2 = M_0/(l\hat{B}_{th}^2 N_A^{2/3}) \quad (17a)$$

$$\nu = bl^2 c_{th}/c^{**} \quad (17b)$$

$$c^{**} = M_0/(lb^2 N_A) \quad (17c)$$

Finally, to determine whether to use the Kavassalis−Noolandi or Rubinstein−Colby conjecture for entanglements, we inspect the dimensionless parameter $c_{th}b^3 N_A M_0^{-1}$. If this quantity is less than unity, the solvent is considered marginally good, and the Rubinstein−Colby method is applied (see the Supporting Information, Section S1). If it is greater than unity, the Kavassalis−Noolandi conjecture is applied as described in the previous section.

https://doi.org/10.1021/acspolymersau.1c00028
ACS Polym. Au 2021, 1, 196−205

Table 1. Summary of Parameters of Studied Systems

system	symbol	T [K]	M_w [kg/mol]	M_0 [g/mol]	l [nm]	$\hat{B}_g$ [c]	$\hat{B}_{th}$ [c]	c^* [g/L]	c_{th} [g/L]	c^{**} [g/L]	D_{th} [nm]	b [nm]	v [nm^3]	$c_{th}b^3N_AM_0^{-1}$	$\tilde{P}_e$
Galactomannan - Guar Gum, Water, salt not reported [48]	◆	Not Reported	3192 [a]	265.91	0.54		9.82	0.53		15.95		7.16			6.5
	◆		1120					0.89							
	◆		665 [a]					1.16							
	◆		510					1.33							
	◆		252.7 [a]					1.88							
Galactomannan - *M. flocculosa*, Water, salt not reported [38]	⬟	298	1485.5	310.90	0.54	31.23	10.99	0.59	3.51	21.39	40.7	6.69	0.32	2.03	3.3
Galactomannan - *M. bimucronata*, Water, salt not reported [38]	⬟		1078.0	316.56		31.97	10.40	0.80	1.90	16.82	67.5	7.61	0.25	1.59	7.2
Galactomannan - *M. aspericarpa*, Water, salt not reported [38]	⬟		593.5	306.91		31.17	10.81	1.18	3.09	20.31	44.8	6.82	0.30	1.92	5.8
Galactomannan – *M. taimbensis*, Water, salt not reported [38]	⬟		502.5	301.92		31.30	10.79	1.35	2.96	20.47	46.6	6.73	0.28	1.80	7.6
Galactomannan - *Cassia nodosa*, Water, salt not reported [42]	■	298	701	207.82	0.54		7.68	0.54		7.65		9.14			7.2
Chitosan, Water, 0.3M Acetic Acid, 0.05M AcONa [36]	●	298	193 [b]	165.26	0.54	20.08	7.68	0.74	1.93	9.61	36.2	7.27	0.43	2.71	12.7
	●	278				18.89	7.05	0.62	1.29	6.81	45.6	8.64	0.48	3.03	
Sodium Hyaluronate, Water, 0.1M NaCl [37]	★	298	2200	401.30	0.99	24.57		0.20							3.7
	★		1350					0.31							
	★		1000					0.39							
	★		390 [a]					0.79							
	★		250 [a]					1.11							
Sodium Hyaluronate, Water, pH 7.0, 0.15M NaCl [46]	⬢	298	4000	401.30	0.99	24.23		0.13							
	⬢		1250 [a]					0.31							
Sodium Hyaluronate, Water, pH 13.2, 0.15M NaCl [46]	⬢	298	1600	401.30	0.99	40.02		1.17							3.2
Sodium Hyaluronate, Water, pH 7.0, 0.015M NaCl [46]	⬢	298	1600	401.30	0.99	21.74		0.19							
Sodium Hyaluronate, PBS, 0.138M NaCl, 0.0027M KCl [53]	⬢	298	1500	401.30	0.99	25.41		0.31							
Sodium Carboxymethyl Cellulose, Water, 0.1M NaCl [47]	■	293	190	234.16	0.54	21.87	8.34	0.97	2.43	9.43	33.9	8.74	0.66	4.17	9.6
Sodium Alginate, Water, 0.1M NaCl [47]	■	293	100	396.22	1.08	23.64		2.00							3.6
Hydroxypropyl Methyl Cellulose, Water, 0.1M NaCl [47]	■	293	430	188.49	0.54	20.49		0.43							3.0
Methyl Cellulose, Water, 0.1M NaCl [47]	■	293	230	191.60	0.54	20.86		0.73							3.4
Sodium κ-carrageenan, Water, 0.1M NaCl [47]	▲	293	530	408.31	0.99	25.92	9.44	0.74	2.70	16.25	39.0	6.49	1.06	1.09	10.8
Sodium κ-carrageenan, Water, 0.1M NaCl [54]	▲		430					0.87							
Hydroxypropyl Cellulose, Water, salt not reported [57]	▲	298	2500	393	0.54	37.30		0.67							2.7
	▲		700	411		36.75		1.70							2.9
	▲		180	387		36.58		4.73							3.4
Hydroxyethyl Cellulose, Water, 0.1M NaCl [34]	◀	298	457 [b]	233.07	0.54		7.81	0.71		7.30		9.91			9.7
Xanthan gum, Water, 0.05M NaCl [55]	▽	298	2000	Not Reported	1.08	14.65		0.05							4.4
Xanthan gum, Water, 0.1M NaCl [44]	▼	298	7000	869.86	1.08	24.20		0.08							2.6
Apple pectin, Water, 3.1×10^{-4}M NaN_3 and 0.2M NaCl [39]	▶	298	459	192.84	0.54	37.64	13.04	2.52	5.36	68.31	37.5	2.95	0.067	0.43	8.7
	▶		490	204.16	0.54			2.40		64.53		3.12	0.076	0.48	8.3
Cellulose tris(phenyl carbamate), THF [56]	○	298	450 [a]	519.51	0.54	39.83		3.03							3.4
	○		232					4.75							
	○		150					7.02							
	○		78 [a]					11.57							
	○		58 [a]					14.50							
	○		35 [a]					21.33							
	○		15 [a]					40.76							

[a]Indicated values of M_w are adjusted to be consistent with other molecular weights in the same system (see Supporting Information Section S2). [b]Indicated values of M_w are viscosity-average molecular weight, as reported in the reference. Values of M_0 are calculated according to the procedure outlined in the Supporting Information, Section S3. [c]Dimensions of $\hat{B}_g$ and $\hat{B}_{th}$ are $(mol/L)^{1/3}(g/mol)^{0.588}$ and $(mol/L)^{1/3}(g/mol)^{1/2}$, respectively. Values of c^* are calculated from eq 15. Values of c_{th} are calculated from eq 16. Values of D_{th} are calculated with eq 13 at $c = c_{th}$. Values of c^{**}, b, and v are calculated using eqs 17 with the values of M_0 and l given in the table. For the apple pectin systems, the reported value of the packing number is $\tilde{P}_e = \tilde{P}_{e,RC}(c_{th}b^3N_AM_0^{-1})^{-1/3}$, where $\tilde{P}_{e,RC}$ is the fitting parameter estimated for the fit to eq 10 in Figure 3f.

To determine the values of the $\hat{B}$-parameters, we note that in the Rouse (unentangled solution) regime, $M_w/M_e < 1$ (see eq 8), the solution specific viscosity

$$\eta_{sp} = M_w/M_g \tag{18}$$

and scales with concentration as $c^{1/(3\nu-1)}$, where the exponent ν is determined by the statistics of the chain on the length scale of the correlation blob. Therefore, we can use a normalized specific viscosity $\eta_{sp}/M_wc^{1/(3\nu-1)}$ to find the plateau or minimum value $\hat{C}_p$ corresponding to different solution concentration regimes and to obtain values of the $\hat{B}$-parameters as follows

$$\hat{B} = \hat{C}_p^{1/3-\nu} \tag{19}$$

Below, we illustrate this approach by determining $\hat{B}$-parameters for solutions of sodium carboxymethyl cellulose and apple pectin.

The first example corresponds to 0.1 M NaCl aqueous solutions of sodium carboxymethyl cellulose at a temperature of 293 K and weight-average molecular weight $M_w = 1.9 \times 10^5$ g/mol,[47] shown in Figure 3. The degree of substitution of sodium carboxymethyl groups in place of hydroxyl groups can be determined experimentally through elemental analysis (see chemical structure in the Supporting Information, Table S3). Using the reported degree of substitution DS = 0.9, we estimate a repeat unit molar mass of $M_0 = 234.16$ g/mol. The concentration dependence of the specific viscosity is presented in Figure 3a. The normalized specific viscosity data shown in Figure 3b and Figure 3c are used to obtain $\hat{C}_{p,g} = 5.48 \times 10^{-6}$ $(mol/g)(L/g)^{1.31}$ and $\hat{C}_{p,th} = 2.97 \times 10^{-6}$ $(mol/g)(L/g)^2$, respectively. The concentration dependence of the normalized specific viscosity $\eta_{sp}/M_wc^{3/(3\nu-1)} = \eta_{sp}/M_wc^{3.93}$ (where $\nu = 0.588$) is shown in Figure 3d. The clear increase at higher concentrations indicates that the solution crosses over to the thermal blob overlap regime and therefore suggests that the plateau value $\hat{C}_{p,th}$ can be used to determine the parameter $\hat{B}_{th}$. With these plateau values, we use eq 19 to calculate $\hat{B}_g = 21.87(mol/L)^{1/3}(g/mol)^{0.588}$ and $\hat{B}_{th} = 8.34$ $(mol/L)^{1/3}(g/mol)^{1/2}$. All values of $\hat{B}$ obtained from the plateau values $\hat{C}_p$ are given in Table 1.

In this system, the parameter $c_{th}b^3N_AM_0^{-1}$ is 4.2 (greater than unity), signifying we can use the Kavassalis–Noolandi conjecture to calculate $\tilde{P}_e$ and M_e. Figure 3f shows the fit of the normalized solution

https://doi.org/10.1021/acspolymersau.1c00028
ACS Polym. Au 2021, 1, 196–205

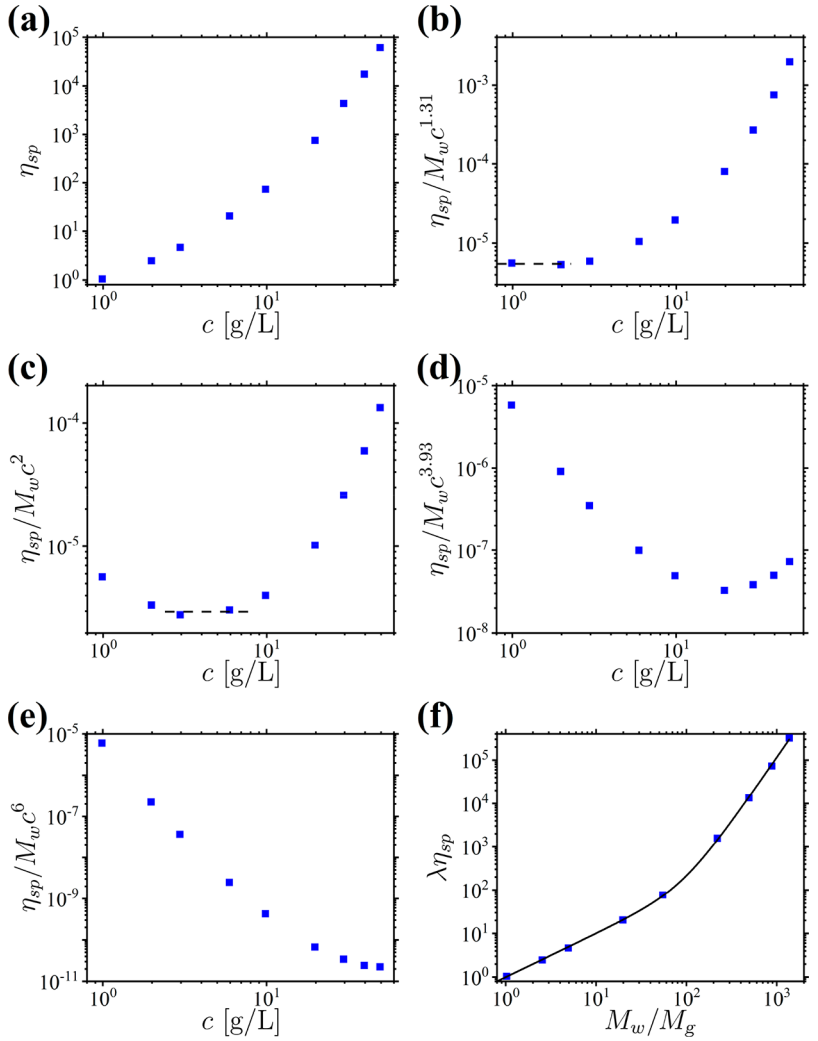

Figure 3. Dependence of the solution specific viscosity (a), $\eta_{sp}/M_w c^{1.31}$ (b), $\eta_{sp}/M_w c^2$ (c), $\eta_{sp}/M_w c^{3.93}$ (d), and $\eta_{sp}/M_w c^6$ (e) on concentration c in grams per liter for solutions of sodium carboxymethyl cellulose in 0.1 M NaCl aqueous solutions from ref 47. Dashed line in (b) corresponds to estimated value of $\hat{C}_{p,g} = 5.48 \times 10^{-6}$ (mol/g)(L/g)$^{1.31}$. Dashed line in (c) corresponds to estimated value of $\hat{C}_{p,th} = 2.97 \times 10^{-6}$ (mol/g)(L/g)^2. (f) Dependence of normalized specific viscosity $\lambda\eta_{sp}$ on M_w/M_g. Solid line is best fit to eq 10.

viscosity data dependence on M_w/M_g to eq 10 with fitting parameter $\tilde{P}_e = 9.6$.

The second data set corresponds to two solutions of apple pectin with weight-average molecular weights of 4.59×10^5 and 4.90×10^5g/mol,[39] with the original specific viscosity data plotted in Figure 4a. Here, we will refer to the apple pectin sample with M_w equal to 4.59×10^5g/mol as "sample I" and the sample with M_w equal to 4.90×10^5g/mol as "sample II" (weight fractions of neutral sugars and functional groups in these samples can be found in ref 39). According to the gas chromatography results reported in the source material, the weight fraction of component sugar units and the degree of methyl substitution on the repeat unit are very similar between the samples, differing by less than 3%, which indicates that their values of $\hat{B}_g$ and $\hat{B}_{th}$ should be almost indistinguishable. As such, the plateaus for sample II were used in Figures 4b and Figure 4c, obtaining $\hat{C}_{p,g} = 6.50 \times 10^{-7}$ (mol/g)(L/g)$^{1.31}$ and $\hat{C}_{p,th} = 2.04 \times 10^{-7}$ (mol/g)(L/g)^2. As with the previous example, the chains do not entangle at concentrations below the thermal blob overlap concentration, as there is no plateau in Figure 4d. Therefore, we use eq 19 again to calculate $\hat{B}_g = 37.64$ (mol/L)$^{1/3}$(g/mol)$^{0.588}$ and $\hat{B}_{th} = 13.04$ (mol/L)$^{1/3}$(g/mol)$^{1/2}$. The results of this analysis are reported in Table 1.

The values of the parameter $c_{th}b^3N_AM_0^{-1}$ in sample I and sample II are 0.43 and 0.48, respectively, which are both less than unity, so the Rubinstein–Colby conjecture has to be used to calculate entanglement molecular weight $\tilde{M}_e$ (explained in the Supporting Information, Section S1). The fitting parameter for eq 10 used on the basis of the Rubinstein–Colby conjecture $\tilde{P}_{e,RC}$, is estimated to be 6.5. The actual packing number is calculated with the equation $\tilde{P}_e = \tilde{P}_{e,RC}(c_{th}b^3N_AM_0^{-1})^{-1/3}$ giving values of 8.7 for sample I and 8.3 for sample II. The small difference in $\tilde{P}_e$ for the samples is due to the different repeat unit molar masses. The collapse of both data sets in both the Rouse and entangled solution regimes stands as a final confirmation for the obtained values of the $\hat{B}$-parameters for both samples.

It is worthy to mention that while the data used in this analysis of polysaccharide solutions are considered semidilute, they are well below concentrated solution regimes. All concentrations of polysaccharide solutions studied here are below approximately 10% of the bulk densities. The elimination of concentrations nearing the bulk density makes this analysis more reliable in two ways: (i) it eliminates viscosity data that may be influenced by shear thinning, and (ii) it eliminates the need for the corrections that viscosity measurements may require due to proximity to the glass transition temperature.

The triplet $\{B_g, B_{th}, \tilde{P}_e\}$ of the dimensionless parameters describes both static and dynamic properties of solutions by allowing calculations of concentration dependence of the solution correlation length ξ and of the degree of polymerization between entanglements $\tilde{N}_e$. Creating a library of polymer/solvent pairs with associated triplets would enable investigations into the principal components of a system

https://doi.org/10.1021/acspolymersau.1c00028
ACS Polym. Au 2021, 1, 196–205

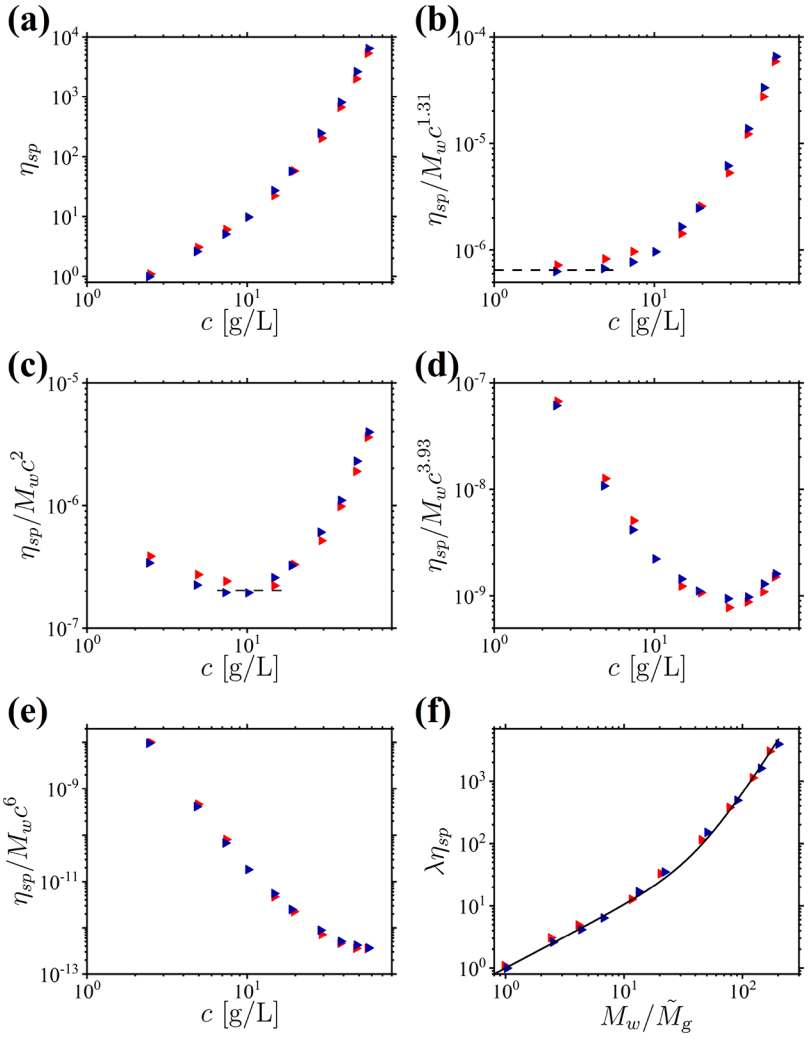

Figure 4. Dependence of the solution specific viscosity (a), $\eta_{sp}/M_w c^{1.31}$ (b), $\eta_{sp}/M_w c^2$ (c), $\eta_{sp}/M_w c^{3.93}$ (d), and $\eta_{sp}/M_w c^6$ (e) on concentration c in grams per liter for 3.1×10^{-4} M NaN_3 and 0.2 M NaCl aqueous solutions of apple pectin from ref 39. Dashed line in (b) corresponds to estimated value of $\hat{C}_{p,g} = 6.50 \times 10^{-7}$ (mol/g)(L/g)$^{1.31}$. Dashed line in (c) corresponds to estimated value of $\hat{C}_{p,th} = 2.04 \times 10^{-7}$ (mol/g)(L/g)^2. (f) Dependence of normalized specific viscosity $\lambda\eta_{sp}$ on $M_w/\tilde{M}_g$. Solid line is best fit to eq 10. See Table 1 for symbol notations.

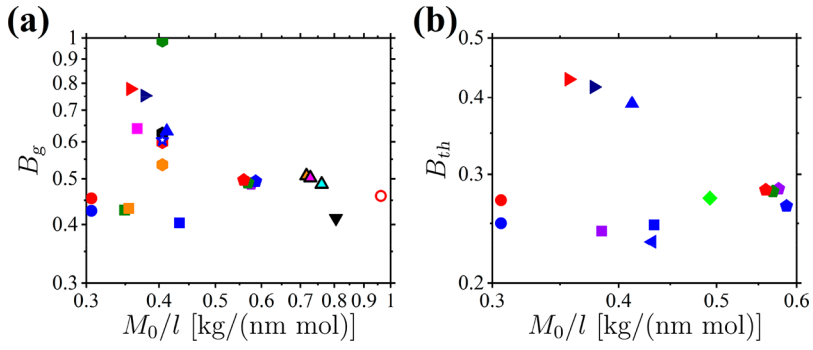

Figure 5. Dependence of the dimensionless parameters (a) B_g and (b) B_{th} on repeat unit linear mass density M_0/l. Symbol notations are summarized in Table 1.

that uniquely determine a triplet, which may include the linear mass density M_0/l or the Fixman swelling ratio[67] $\alpha^2 = \langle R^2\rangle/blN$.

Figure 5 represents dimensionless B-parameters given by eq 14 as functions of linear mass density M_0/l for the studied systems. It is important to remember that smaller values of the B_g parameter correspond to better solvent conditions for the polymer backbone (see eq 3). In particular, systems with B_g values in the range of 0.4–0.5 (see Figure 5a) show no dependence on the linear mass density: 0.1 M NaCl aqueous solutions of hydroxypropyl methyl cellulose (green square), methyl cellulose (orange square), sodium carboxymethyl cellulose (blue square), and xanthan gum (black inverted triangle), as well as aqueous solutions of galactomannan with an unreported ionic strength (pentagons), aqueous acetic acid solutions of chitosan (circles), tetrahydrofuran solutions of cellulose tris(phenyl carbamate) (hollow circle), and aqueous solutions of hydroxypropyl cellulose (outlined triangles). Similarly, 0.1 M NaCl aqueous solutions

https://doi.org/10.1021/acspolymersau.1c00028
ACS Polym. Au 2021, 1, 196–205

of sodium alginate (pink square), sodium κ-carrageenan (blue triangle), and sodium hyaluronate (black and red hexagons and blue star) are clustered near $B_g = 0.6$. The spread of the other sodium hyaluronate systems (hexagons) can be attributed to a higher solution pH (green) or a lower ionic strength (orange). Similarly, the apple pectin systems (right triangles) with a higher ionic strength (0.2 M NaCl) have much larger values of B_g, and the chitosan systems with a much lower pH (0.3 M acetic acid) have much smaller values. The effects of temperature on solvent quality can also be seen for the chitosan systems, where a temperature increase from 278 K (blue circle) to 298 K (red circle) increases the value of the B_g parameter.

In Figure 5b, the B_{th} values for chitosan, sodium carboxymethyl cellulose, hydroxyethyl cellulose, and all galactomannan systems stay within 0.23−0.3. The values for the two apple pectin systems and the sodium κ-carrageenan systems are noticeably larger. Note that the value of the B_{th} parameter is inversely proportional to square root of the number of repeat units per Kuhn length (see eq 4), and thus stiffer polymers have smaller values of this parameter. With this data representation, we hope to inspire studies of the effects of solvent, temperature, salt content and valence, and degree of substitution of functional groups on the interaction parameters.

We can use the B-parameters shown in Figures 5a and b to construct a universal diagram of states of different solution regimes implementing a 2-D data representation in terms of the dimensionless excluded volume v/bl^2 (see eq 17b) and dimensionless concentration c/c^{**} as shown in Figure 6. Each polymer/solvent pair is shown as a horizontal line. The solvent quality for a polymer improves with an increasing value of the parameter v/bl^2. For a given polymer/solvent pair, there is a point on the line for the corresponding value of c^*/c^{**} for each molecular weight studied, describing a crossover to the semidilute solution regime. For comparison we have also added data sets corresponding to synthetic polymers studied previously,[50,51] shown as black half-filled symbols (poly(ethylene oxide) in water,[68] polystyrene in toluene,[69,70] poly(methyl methacrylate) in ionic liquids [C_4(mim)][TFSI] and [C_8(mim)$_2$][TFSI]$_2$,[71] and poly(2-vinylpyridine) in ethylene glycol).[72] We would like to emphasize that the approach developed here only allows for the representation of systems for which the location of the crossover concentration c_{th} falls within the studied concentration range and is below the concentrated solution regime ($c_{th} < c^{**}$). This corresponds to values of the dimensionless parameter $v/bl^2 < 1$. If it is impossible to identify a location of c_{th} from the analysis of the solution viscosity of a polymer in a good solvent, this indicates that for such a system $v/bl^2 > 1$ and the thermal blob size D_{th} is smaller than the Kuhn length, b. Conversely, if the polymer is in a θ solvent in the entire semidilute concentration regime, then for the largest molecular weight studied, $c_{th} < c^*$, and therefore $v/bl^2 < c^*/c^{**}$.

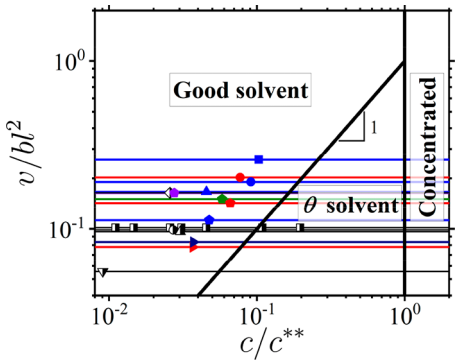

Figure 6. Diagram of different solution regimes in terms of v/bl^2 and c/c^{**}. Symbols indicate location of polymer overlap concentration c^*/c^{**} for studied degrees of polymerization. Symbol notations for solutions of biopolymers are summarized in Table 1. Data sets corresponding to solutions of synthetic polymers are given by black half-filled symbols: poly(2-vinylpyridine) in ethylene glycol (circle, $M_w = 3.64 \times 10^5$ g/mol), poly(methyl methacrylate) in ionic liquids [C_4(mim)][TFSI] (rhomb) and [C_8(mim)$_2$][TFSI]$_2$ (triangle) ($M_w = 3.061 \times 10^5$ g/mol), aqueous solutions of poly(ethylene oxide) (inverted triangle, $M_w = 4.0 \times 10^5 - 4.0 \times 10^6$ g/mol), and polystyrene in toluene (squares, $M_w = 1.5 \times 10^4 - 2.36 \times 10^7$ g/mol).

The reduced viscosity $\lambda\eta_{sp}/\tilde{P}_e^2$ for all studied systems are shown in Figure 7 as a function of the effective number of entanglements per chain, $M_w/\tilde{M}_e$. The data collapse into one universal curve, given by the equation

$$\lambda\eta_{sp}/\tilde{P}_e^2 = M_w/\tilde{M}_e(1 + (M_w/\tilde{M}_e)^2) \quad (20)$$

confirming universality in the chain dynamics at different solution regimes. Note that, at a large number of entanglements per chain, the data deviates from the predicted power law of $\eta_{sp} \sim (M_w/\tilde{M}_e)^3$ and toward a scaling dependence of $\eta_{sp} \sim (M_w/\tilde{M}_e)^{3.4}$. This stronger dependence is attributed to tube length fluctuations.[49,73]

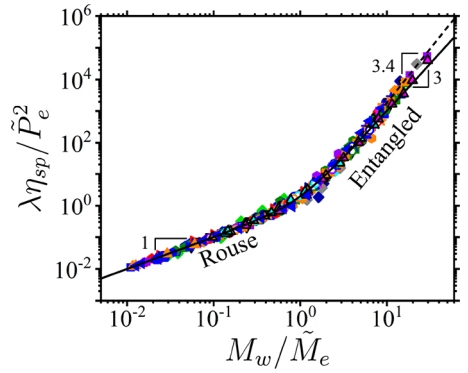

Figure 7. Dependence of normalized specific viscosity $\lambda\eta_{sp}/\tilde{P}_e^2$ on the number of entanglements per chain $M_w/\tilde{M}_e$ for all studied systems. Symbol notations are summarized in Table 1. Solid line is given by eq 20, and dashed line corresponds to a slope of 3.4.

CONCLUSIONS

We have presented a scaling-based approach to obtain $\hat{B}$-parameters in different concentration regimes of polysaccharide solutions. In particular, these parameters were obtained from the concentration dependence of the normalized solution specific viscosity, $\eta_{sp}/M_w\ c^{1/(3\nu-1)}$, in the different solution regimes as illustrated in Figure 3 and Figure 4. The $\hat{B}$-parameters were used to describe chain entanglements by applying the Kavassalis−Noolandi conjecture[60−62] in good solvents or the Rubinstein−Colby conjecture[63−65] in θ or marginally good solvents.

A map of the dimensionless B-parameters and the linear mass density shown in Figures 5 correlates the molecular structure of polysaccharides and the typical scale of the interaction parameters. This information can also be used to highlight correlations between molecular parameters such as Kuhn length, excluded volume and thermal blob size, and system parameters such as linear mass density M_0/l, solution temperature and salt concentration (see Table 1). Furthermore, we used the information summarized in Table 1 to construct a universal diagram of states of different solution regimes (see Figure 6). This data representation allows us to establish the relative solvent quality for different polymer systems. In particular, larger values of the dimensionless parameter v/bl^2 correspond to better solvent quality for a polymer.

Finally, the collapse of the data in Figure 7 highlights the universality of the specific viscosity in both the Rouse and

https://doi.org/10.1021/acspolymersau.1c00028
ACS Polym. Au 2021, 1, 196−205

entangled solution regimes as a function of $M_w/\tilde{M}_e$ and serves as a final confirmation that our calculations of the $\hat{B}$-parameters for different polysaccharides are correct.

The approach developed here can also be used to analyze the concentration dependence of the diffusion coefficient,[74−76] osmotic pressure,[77−79] and relaxation time[80] in semidilute solutions of biopolymers. Furthermore, the B-parameters can be used to create a database of systems that can form the basis for a machine learning approach[81−84] to biopolymer solutions. This information can also be used to predict concentration dependence of the solution viscosity of polysaccharides of a particular molecular weight. We hope that this work will encourage future research in this direction.

■ ASSOCIATED CONTENT

Supporting Information

The Supporting Information is available free of charge at https://pubs.acs.org/doi/10.1021/acspolymersau.1c00028.

List of notations, calculations of N_e, molecular weight adjustment, repeat unit molar mass calculations, and data analysis of polysaccharide systems (PDF)

■ AUTHOR INFORMATION

Corresponding Author

Andrey V. Dobrynin − *Department of Chemistry, University of North Carolina, Chapel Hill, North Carolina 27599, United States;* orcid.org/0000-0002-6484-7409; Email: avd@email.unc.edu

Authors

Ryan Sayko − *Department of Chemistry, University of North Carolina, Chapel Hill, North Carolina 27599, United States;* orcid.org/0000-0002-5986-4829

Michael Jacobs − *Department of Chemistry, University of North Carolina, Chapel Hill, North Carolina 27599, United States;* orcid.org/0000-0002-7255-3451

Complete contact information is available at: https://pubs.acs.org/10.1021/acspolymersau.1c00028

Notes

The authors declare no competing financial interest.

■ ACKNOWLEDGMENTS

This work was supported by the National Science Foundation under Grant DMREF-2049518.

■ REFERENCES

(1) Dumitriu, S. *Polysaccharides: Structural Diversity and Functional Versatility*; CRC Press: New York, 2004.

(2) Cantor, C. R.; Schimmel, P. R. *Biophysical Chemistry Part I: The conformation of biological macromolecules*; W. H. Freeman and Company: San Francisco, 1980.

(3) Rinaudo, M.; Pavlov, G.; Desbrières, J. Influence of acetic acid concentration on the solubilization of chitosan. *Polymer* **1999**, *40* (25), 7029−7032.

(4) Sorlier, P.; Denuzière, A.; Viton, C.; Domard, A. Relation between the Degree of Acetylation and the Electrostatic Properties of Chitin and Chitosan. *Biomacromolecules* **2001**, *2* (3), 765−772.

(5) Kasabo, F.; Kanematsu, T.; Nakagawa, T.; Sato, T.; Teramoto, A. Solution Properties of Cellulose Tris(phenyl carbamate). 1. Characterization of the Conformation and Intermolecular Interaction. *Macromolecules* **2000**, *33* (7), 2748−2756.

(6) Vårum, K. M.; Ottøy, M. H.; Smidsrød, O. Water-solubility of partially N-acetylated chitosans as a function of pH: effect of chemical composition and depolymerisation. *Carbohydr. Polym.* **1994**, *25* (2), 65−70.

(7) Yalpani, M.; Hall, L. D. Some chemical and analytical aspects of polysaccharide modifications. III. Formation of branched-chain, soluble chitosan derivatives. *Macromolecules* **1984**, *17* (3), 272−281.

(8) Antoniou, E.; Tsianou, M. Solution properties of dextran in water and in formamide. *J. Appl. Polym. Sci.* **2012**, *125* (3), 1681−1692.

(9) Kobayashi, K.; Huang, C.-i.; Lodge, T. P. Thermoreversible Gelation of Aqueous Methylcellulose Solutions. *Macromolecules* **1999**, *32* (21), 7070−7077.

(10) Li, Y.; Liu, P.; Ma, C.; Zhang, N.; Shang, X.; Wang, L.; Xie, F. Structural Disorganization and Chain Aggregation of High-Amylose Starch in Different Chloride Salt Solutions. *ACS Sustainable Chem. Eng.* **2020**, *8* (12), 4838−4847.

(11) Ganesan, M.; Knier, S.; Younger, J. G.; Solomon, M. J. Associative and Entanglement Contributions to the Solution Rheology of a Bacterial Polysaccharide. *Macromolecules* **2016**, *49* (21), 8313−8321.

(12) Ganesan, M.; Stewart, E. J.; Szafranski, J.; Satorius, A. E.; Younger, J. G.; Solomon, M. J. Molar mass, entanglement, and associations of the biofilm polysaccharide of Staphylococcus epidermidis. *Biomacromolecules* **2013**, *14* (5), 1474−1481.

(13) Wang, H.; Qian, J.; Ding, F. Emerging Chitosan-Based Films for Food Packaging Applications. *J. Agric. Food Chem.* **2018**, *66* (2), 395−413.

(14) Cazón, P.; Vázquez, M. Bacterial cellulose as a biodegradable food packaging material: A review. *Food Hydrocolloids* **2021**, *113*, 106530.

(15) Nechita, P.; Roman, M. Review on Polysaccharides Used in Coatings for Food Packaging Papers. *Coatings* **2020**, *10* (6), 566.

(16) Gupta, N. R.; Torris, A. T. A.; Wadgaonkar, P. P.; Rajamohanan, P. R.; Ducouret, G.; Hourdet, D.; Creton, C.; Badiger, M. V. Synthesis and characterization of PEPO grafted carboxymethyl guar and carboxymethyl tamarind as new thermo-associating polymers. *Carbohydr. Polym.* **2015**, *117*, 331−338.

(17) García-Ochoa, F.; Santos, V. E.; Casas, J. A.; Gómez, E. Xanthan gum: production, recovery, and properties. *Biotechnol. Adv.* **2000**, *18* (7), 549−579.

(18) Li, Q.; Wang, S.; Jin, X.; Huang, C.; Xiang, Z. The Application of Polysaccharides and Their Derivatives in Pigment, Barrier, and Functional Paper Coatings. *Polymers (Basel, Switz.)* **2020**, *12* (8), 1837.

(19) Laine, C.; Harlin, A.; Hartman, J.; Hyvärinen, S.; Kammiovirta, K.; Krogerus, B.; Pajari, H.; Rautkoski, H.; Setälä, H.; Sievänen, J.; Uotila, J.; Vähä-Nissi, M. Hydroxyalkylated xylans − Their synthesis and application in coatings for packaging and paper. *Ind. Crops Prod.* **2013**, *44*, 692−704.

(20) Azeredo, H. M. C.; Barud, H.; Farinas, C. S.; Vasconcellos, V. M.; Claro, A. M. Bacterial Cellulose as a Raw Material for Food and Food Packaging Applications. *Frontiers in Sustainable Food Systems* **2019**, 3 (7) DOI: 10.3389/fsufs.2019.00007.

(21) Croisier, F.; Jérôme, C. Chitosan-based biomaterials for tissue engineering. *Eur. Polym. J.* **2013**, *49* (4), 780−792.

(22) Rehm, B. H. A.; Valla, S. Bacterial alginates: biosynthesis and applications. *Appl. Microbiol. Biotechnol.* **1997**, *48* (3), 281−288.

(23) Mazur, K.; Buchner, R.; Bonn, M.; Hunger, J. Hydration of Sodium Alginate in Aqueous Solution. *Macromolecules* **2014**, *47* (2), 771−776.

(24) Chou, T. D.; Kokini, J. L. Rheological Properties and Conformation of Tomato Paste Pectins, Citrus and Apple Pectins. *J. Food Sci.* **1987**, *52* (6), 1658−1664.

(25) Clark, A. H.; Gidley, M. J.; Richardson, R. K.; Ross-Murphy, S. B. Rheological studies of aqueous amylose gels: the effect of chain length and concentration on gel modulus. *Macromolecules* **1989**, *22* (1), 346−351.

(26) Doublier, J. L.; Launay, B. Rheology of Galactomannan Solutions: Comparative Study of Guar Gum and Locust Bean Gum. *J. Texture Stud.* **1981**, *12* (2), 151−172.
(27) Kesavan, S.; Prud'homme, R. K. Rheology of guar and (hydroxypropyl) guar crosslinked by borate. *Macromolecules* **1992**, *25* (7), 2026−2032.
(28) Oviatt, H. W.; Brant, D. A. Viscoelastic Behavior of Thermally Treated Aqueous Xanthan Solutions in the Semidilute Concentration Regime. *Macromolecules* **1994**, *27* (9), 2402−2408.
(29) Philippova, O. E.; Shibaev, A. V.; Muravlev, D. A.; Mityuk, D. Y. Structure and Rheology of Solutions and Gels of Stiff Polyelectrolyte at High Salt Concentration. *Macromolecules* **2016**, *49* (16), 6031−6040.
(30) Richardson, P. H.; Clark, A. H.; Russell, A. L.; Aymard, P.; Norton, I. T. Galactomannan Gelation: A Thermal and Rheological Investigation Analyzed Using the Cascade Model. *Macromolecules* **1999**, *32* (5), 1519−1527.
(31) Westra, J. G. Rheology of carboxymethyl cellulose with xanthan gum properties. *Macromolecules* **1989**, *22* (1), 367−370.
(32) Wientjes, R. H. W.; Duits, M. H. G.; Jongschaap, R. J. J.; Mellema, J. Linear Rheology of Guar Gum Solutions. *Macromolecules* **2000**, *33* (26), 9594−9605.
(33) Bell, A. E.; Allen, A.; Morris, E. R.; Ross-Murphy, S. B. Functional interactions of gastric mucus glycoprotein. *Int. J. Biol. Macromol.* **1984**, *6* (6), 309−315.
(34) Castelain, C.; Doublier, J. L.; Lefebvre, J. A study of the viscosity of cellulose derivatives in aqueous solutions. *Carbohydr. Polym.* **1987**, *7* (1), 1−16.
(35) Cuvelier, G.; Launay, B. Concentration regimes in xanthan gum solutions deduced from flow and viscoelastic properties. *Carbohydr. Polym.* **1986**, *6* (5), 321−333.
(36) Desbrieres, J. Viscosity of Semiflexible Chitosan Solutions: Influence of Concentration, Temperature, and Role of Intermolecular Interactions. *Biomacromolecules* **2002**, *3* (2), 342−349.
(37) Fouissac, E.; Milas, M.; Rinaudo, M. Shear-rate, concentration, molecular weight, and temperature viscosity dependences of hyaluronate, a wormlike polyelectrolyte. *Macromolecules* **1993**, *26* (25), 6945−6951.
(38) Ganter, J. L. M. S.; Reicher, F. Water-soluble galactomannans from seeds of Mimosaceae spp. *Bioresour. Technol.* **1999**, *68* (1), 55−62.
(39) Hwang, J.; Kokini, J. L. Contribution of the side branches to rheological properties of pectins. *Carbohydr. Polym.* **1992**, *19* (1), 41−50.
(40) Ioan, C. E.; Aberle, T.; Burchard, W. Light Scattering and Viscosity Behavior of Dextran in Semidilute Solution. *Macromolecules* **2001**, *34* (2), 326−336.
(41) Hwang, J. K.; Shin, H. H. Rheological properties of chitosan solutions. *Korea-Australia Rheology Journal* **2000**, *12* (3/4), 175−179.
(42) Kapoor, V. P.; Milas, M.; Taravel, F. R.; Rinaudo, M. Rheological properties of seed galactomannan from Cassia nodosa buch.-hem. *Carbohydr. Polym.* **1994**, *25* (2), 79−84.
(43) Meadows, J.; Williams, P. A.; Kennedy, J. C. Comparison of the extensional and shear viscosity characteristics of aqueous hydroxyethyl cellulose solutions. *Macromolecules* **1995**, *28* (8), 2683−2692.
(44) Milas, M.; Rinaudo, M.; Tinland, B. The viscosity dependence on concentration, molecular weight and shear rate of xanthan solutions. *Polym. Bull.* **1985**, *14* (2), 157−164.
(45) Morris, E. R.; Cutler, A. N.; Ross-Murphy, S. B.; Rees, D. A.; Price, J. Concentration and shear rate dependence of viscosity in random coil polysaccharide solutions. *Carbohydr. Polym.* **1981**, *1* (1), 5−21.
(46) Morris, E. R.; Rees, D. A.; Welsh, E. J. Conformation and dynamic interactions in hyaluronate solutions. *J. Mol. Biol.* **1980**, *138* (2), 383−400.
(47) Potier, M.; Tea, L.; Benyahia, L.; Nicolai, T.; Renou, F. Viscosity of Aqueous Polysaccharide Solutions and Selected Homogeneous Binary Mixtures. *Macromolecules* **2020**, *53* (23), 10514−10525.
(48) Robinson, G.; Ross-Murphy, S. B.; Morris, E. R. Viscosity-molecular weight relationships, intrinsic chain flexibility, and dynamic solution properties of guar galactomannan. *Carbohydr. Res.* **1982**, *107* (1), 17−32.
(49) Rubinstein, M.; Colby, R. H. *Polymer physics*; Oxford University Press: Oxford, 2007.
(50) Dobrynin, A. V.; Jacobs, M.; Sayko, R. Scaling of Polymer Solutions as a Quantitative Tool. *Macromolecules* **2021**, *54* (5), 2288−2295.
(51) Dobrynin, A. V.; Jacobs, M. When Do Polyelectrolytes Entangle? *Macromolecules* **2021**, *54* (4), 1859−1869.
(52) Jacobs, M.; Lopez, C. G.; Dobrynin, A. V. Quantifying the Effect of Multivalent Ions in Polyelectrolyte Solutions. *Macromolecules* **2021**, DOI: 10.1021/acs.macromol.1c01326.
(53) Krause, W. E.; Bellomo, E. G.; Colby, R. H. Rheology of Sodium Hyaluronate under Physiological Conditions. *Biomacromolecules* **2001**, *2* (1), 65−69.
(54) Croguennoc, P.; Meunier, V.; Durand, D.; Nicolai, T. Characterization of Semidilute κ-Carrageenan Solutions. *Macromolecules* **2000**, *33* (20), 7471−7474.
(55) Wyatt, N. B.; Liberatore, M. W. Rheology and viscosity scaling of the polyelectrolyte xanthan gum. *J. Appl. Polym. Sci.* **2009**, *114* (6), 4076−4084.
(56) Sato, T.; Hamada, M.; Teramoto, A. Solution Viscosity of a Moderately Stiff Polymer: Cellulose Tris(phenyl carbamate). *Macromolecules* **2003**, *36* (18), 6840−6843.
(57) Lopez, C. G.; Voleske, L.; Richtering, W. Scaling laws of entangled polysaccharides. *Carbohydr. Polym.* **2020**, *234*, 115886.
(58) De Gennes, P. G. Dynamics of Entangled Polymer Solutions. I. The Rouse Model. *Macromolecules* **1976**, *9* (4), 587−593.
(59) De Gennes, P. G. Dynamics of Entangled Polymer Solutions. II. Inclusion of Hydrodynamic Interactions. *Macromolecules* **1976**, *9* (4), 594−598.
(60) Kavassalis, T. A.; Noolandi, J. New View of Entanglements in Dense Polymer Systems. *Phys. Rev. Lett.* **1987**, *59* (23), 2674−2677.
(61) Kavassalis, T. A.; Noolandi, J. A new theory of entanglements and dynamics in dense polymer systems. *Macromolecules* **1988**, *21* (9), 2869−2879.
(62) Kavassalis, T. A.; Noolandi, J. Entanglement scaling in polymer melts and solutions. *Macromolecules* **1989**, *22* (6), 2709−2720.
(63) Colby, R. H.; Rubinstein, M. Two-parameter scaling for polymers in Θ solvents. *Macromolecules* **1990**, *23* (10), 2753−2757.
(64) Heo, Y.; Larson, R. G. Universal Scaling of Linear and Nonlinear Rheological Properties of Semidilute and Concentrated Polymer Solutions. *Macromolecules* **2008**, *41* (22), 8903−8915.
(65) Milner, S. T. Predicting the Tube Diameter in Melts and Solutions. *Macromolecules* **2005**, *38* (11), 4929−4939.
(66) Morris, E. R.; Ross-Murphy, S. B. *Chain flexibility of polysaccharides and glycoproteins from viscosity measurements*; Elsevier/North-Holland: Shannon Industrial Estate, 1979.
(67) Fixman, M. Excluded Volume in Polymer Chains. *J. Chem. Phys.* **1955**, *23* (9), 1656−1659.
(68) Ebagninin, K. W.; Benchabane, A.; Bekkour, K. Rheological characterization of poly(ethylene oxide) solutions of different molecular weights. *J. Colloid Interface Sci.* **2009**, *336* (1), 360−367.
(69) Kulicke, W. M.; Kniewske, R. The shear viscosity dependence on concentration, molecular weight, and shear rate of polystyrene solutions. *Rheol. Acta* **1984**, *23* (1), 75−83.
(70) Zakin, J. L.; Wu, R.; Luh, H.; Mayhan, K. G. Generalized correlations for molecular weight and concentration dependence of zero-shear viscosity of high polymer solutions. *J. Polym. Sci., Polym. Phys. Ed.* **1976**, *14* (2), 299−308.
(71) He, X.; Kong, M.; Niu, Y.; Li, G. Entanglement and Relaxation of Poly(methyl methacrylate) Chains in Imidazolium-Based Ionic Liquids with Different Cationic Structures. *Macromolecules* **2020**, *53* (18), 7865−7875.
(72) Dou, S.; Colby, R. H. Charge density effects in salt-free polyelectrolyte solution rheology. *J. Polym. Sci., Part B: Polym. Phys.* **2006**, *44* (14), 2001−2013.

(73) Doi, M.; Edwards, S. F. *The theory of polymer dynamics*; Oxford University Press: New York, 1986.
(74) Tirrell, M. Polymer self-diffusion in entangled systems. *Rubber Chem. Technol.* **1984**, *57* (3), 523−556.
(75) Von Meerwall, E. D.; Amis, E. J.; Ferry, J. D. Self-diffusion in solutions of polystyrene in tetrahydrofuran: Comparison of concentration dependences of the diffusion coefficients of polymer, solvent, and a ternary probe component. *Macromolecules* **1985**, *18* (2), 260−266.
(76) Wesson, J. A.; Noh, I.; Kitano, T.; Yu, H. Self-diffusion of polystyrenes by forced Rayleigh scattering. *Macromolecules* **1984**, *17* (4), 782−792.
(77) Cohen, J. A.; Podgornik, R.; Hansen, P. L.; Parsegian, V. A. A Phenomenological One-Parameter Equation of State for Osmotic Pressures of PEG and Other Neutral Flexible Polymers in Good Solvents. *J. Phys. Chem. B* **2009**, *113* (12), 3709−3714.
(78) Kuwahara, N.; Okazawa, T.; Kaneko, M. Excluded-Volume Effect of Polystyrene Solutions. *J. Chem. Phys.* **1967**, *47* (9), 3357−3360.
(79) Noda, I.; Kato, N.; Kitano, T.; Nagasawa, M. Thermodynamic Properties of Moderately Concentrated Solutions of Linear Polymers. *Macromolecules* **1981**, *14* (3), 668−676.
(80) Adam, M.; Delsanti, M. Dynamical behavior of semidilute polymer solutions in a θ solvent: quasi-elastic light scattering experiments. *Macromolecules* **1985**, *18* (9), 1760−1770.
(81) Jordan, M. I.; Mitchell, T. M. Machine learning: Trends, perspectives, and prospects. *Science* **2015**, *349* (6245), 255−260.
(82) Chen, L.; Pilania, G.; Batra, R.; Huan, T. D.; Kim, C.; Kuenneth, C.; Ramprasad, R. Polymer informatics: Current status and critical next steps. *Mater. Sci. Eng., R* **2021**, *144*, 100595.
(83) de Pablo, J. J.; Jones, B.; Kovacs, C. L.; Ozolins, V.; Ramirez, A. P. The Materials Genome Initiative, the interplay of experiment, theory and computation. *Curr. Opin. Solid State Mater. Sci.* **2014**, *18* (2), 99−117.
(84) Audus, D. J.; de Pablo, J. J. Polymer Informatics: Opportunities and Challenges. *ACS Macro Lett.* **2017**, *6* (10), 1078−1082.

https://doi.org/10.1021/acspolymersau.1c00028
ACS Polym. Au 2021, 1, 196−205